

Molecular Sets (MOSES): A Benchmarking Platform for Molecular Generation Models

Daniil Polykovskiy^{1,¶}, Alexander Zhebrak^{1,¶}, Benjamin Sanchez-Lengeling², Sergey Golovanov³, Oktai Tatanov³, Stanislav Belyaev³, Rauf Kurbanov³, Aleksey Artamonov³, Vladimir Aladinskiy¹, Mark Veselov¹, Artur Kadurin^{1,4}, Sergey Nikolenko^{5,3,*}, Alán Aspuru-Guzik^{6,7,8*}, Alex Zhavoronkov^{1,*}

¹ Insilico Medicine, Inc., Johns Hopkins University, 9601 Medical Center Dr, Suite 127 Rockville, MD 20850

² Chemistry and Chemical Biology Department, Harvard University, 12 Oxford Street, Cambridge, Massachusetts 02143, United States

³ Neuromation OU, Tallinn, 10111 Estonia

⁴ Insilico Taiwan, Taipei City 115, Taiwan R.O.C

⁵ National Research University Higher School of Economics, St. Petersburg, 190008, Russia

⁶ Department of Chemistry and Department of Computer Science, University of Toronto, Toronto, Ontario M5S 3H6, Canada

⁷ Vector Institute for Artificial Intelligence, Toronto, Ontario M5S 1M1, Canada

⁸ Biologically-Inspired Solar Energy Program, Canadian Institute for Advanced Research (CIFAR), Toronto, Ontario M5S 1M1, Canada

¶ equal contribution

* corresponding authors

E-mail: alex@insilicomedicine.com, alan@aspuru.com, snikolenko@gmail.com

ABSTRACT

Deep generative models such as generative adversarial networks, variational autoencoders, and autoregressive models are rapidly growing in popularity for the discovery of new molecules and materials. In this work, we introduce MOlecular SEtS (MOSES), a benchmarking platform to support research on machine learning for drug discovery. MOSES implements several popular molecular generation models and includes a set of metrics that evaluate the diversity and quality of generated molecules. MOSES is meant to standardize the research on molecular generation and facilitate the sharing and comparison of new models. Additionally, we provide a large-scale comparison of existing state of the art models and elaborate on current challenges for generative models that might prove fertile ground for new research.

Our platform and source code are freely available at <https://github.com/molecularsets/>.

1. INTRODUCTION

Many challenges of the 21st century, from personalized healthcare to energy production and storage¹, are linked by material discovery and development. The discovery of new molecules can bring enormous societal and technological progress, potentially curing rare diseases and providing a pathway for personalized precision medicine²; disruptive advances are likely to come from unexplored regions of the set of all possible chemical compounds. But a complete exploration of the huge space of potential chemicals is computationally intractable. It has been estimated that the number of

pharmacologically-sensible molecules is in the order of 10^{23} to 10^{80} ^{3,4}. Furthermore, often this search space can be constrained based on known chemistry, patented molecules and desired qualities (e.g. solubility or toxicity). There have been many approaches to mapping and mining the space of possible molecules, including high throughput screening, combinatorial libraries, evolutionary algorithms, and other techniques⁵⁻⁸.

Over the last few years, advances in machine learning, and especially in deep learning have driven the design of new computational systems that improve with experience and are able to model increasingly complex phenomena. One approach that has proven fruitful for the modeling of the distribution of molecular data has been deep generative models. Just as we can sample a random number from a random variable distribution, generative models learn to model a data distribution in a way amenable for sampling new data points or conditioning over certain properties.

Deep generative models have shown remarkable results in a wide range of settings, from generating synthetic images⁹ and natural language texts¹⁰, to the design of DNA sequences¹¹. One important field of application for deep generative models lies in the inverse design of organic molecules¹²: for a given functionality (solubility, ease of synthesizability, toxicity or avoidance of particular molecular fragments, etc.) we wish to find the perfect molecule that meets these requirements. The inverse design uses optimization, sampling, and search methods to navigate the manifold of the functionality of chemical space. A deep generative model fits these requirements since it learns the manifold of desired functionality and allows to map this functionality back to the chemical space.

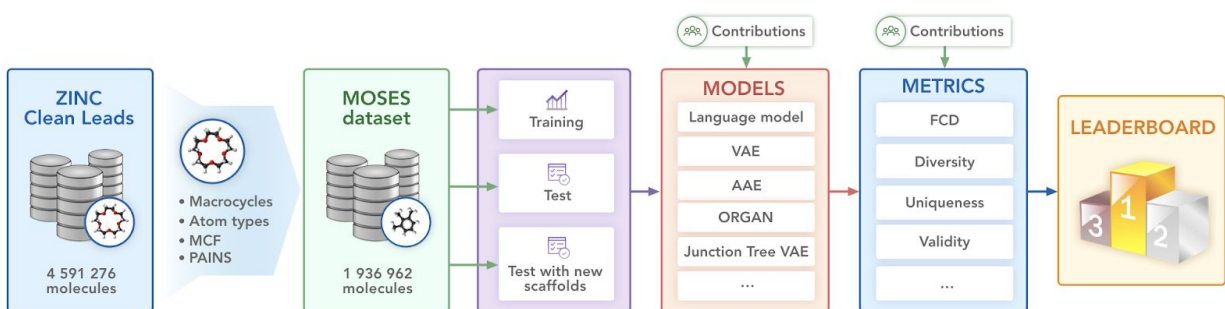


Figure 1. MOSES pipeline. The open-source library provides a dataset, baseline models, and evaluation metrics.

Part of the success of deep learning in different fields has been driven by ever-growing publicly available datasets and standard benchmark sets. These sets serve as a common measuring stick for newly developed models and optimization strategies; for example, when the field of computer vision had more or less worked the classical MNIST dataset of handwritten digits into the ground¹³, larger and more complex datasets such as ImageNet¹⁴ immediately took its place.

In the context of organic molecules, MoleculeNet¹⁵ was introduced as a standardized benchmark suite for discriminative tasks such as regression and classification, but at present, there is no counterpart for generative models and generation tasks. We attribute this due to two main reasons: 1) lack of a common benchmark set and 2) lack of metrics. Both reasons are hard to tackle since any given molecular application will depend highly on context. The molecules used for organic redox flow batteries will differ quite significantly from molecules for Malaria transmission blocking. Even for a common dataset, the

desired qualities might differ greatly. For drug molecules, we sometimes seek a diverse set of molecules to avoid an already patented chemical space, but it can also be advantageous to find molecules that are quite similar in functionality and structure to a patented molecule while being different enough.

Furthermore, it is not immediately clear how to compare deep generative models. There is no clear-cut way to evaluate the quality of generated samples; in particular, the loss function of the model itself is seldom a good choice for final evaluation. Often the real validation test for a candidate sample requires experimental characterization either via multiple in-vitro experiments or a device prototype.

Computational approaches for scoring molecules tend to suffer from a lack of accuracy (e.g., target-ligand interaction) or are too time-consuming (e.g., simulating the electronic structure).

In this work, we aim to tackle both of these problems by providing a unified implementation of a benchmark suite for molecular generation, including data preprocessing utilities, evaluation metrics, and state of the art molecular generation models. While it is clear there can be no single solution to cover all molecular applications, we hope that these contributions will serve as a clear and unified testbed for current and future generative models.

In the following sections, we elaborate on the details of each of the features of MOSES and conclude with evaluation results on a molecular biology dataset along with a discussion on current challenges in molecular generation. We also highlight possible ideas for improvement in datasets outside of a molecular biology context, alternative representations of molecules, and improvements in metrics for the molecules. The pipeline of our framework is shown on Figure 1.

2. DATASET

Deep generative models require large datasets in order to learn patterns that can generalize and lead to new molecules. While large datasets of molecules exist, there is no commonly accepted standard dataset of molecules together with their properties of interest. The pharmaceutical industry has historically driven much of the large-scale development and testing of molecular libraries via virtual screening and high-throughput screening. As Table 1 shows, the largest datasets correspond to libraries utilized in medicinal chemistry. Most publicly available labeled datasets tend to be on the order of 10^2 - 10^4 molecules, which also restricts their utility for data generation tasks, but new techniques and computational screening efforts are paving the way for more applications.

Virtual screening libraries are often constructed from the application of common reactions to a set of seed molecules; the reactions are such that their products are predictable and easily performed in a laboratory setting while seed molecules are typically purchasable or easily synthesized or extracted from natural products. Even though the coverage of reactions tends to be a small subset of all possible reactions¹⁶, the resulting combinations can lead to virtual libraries on the order¹⁷ of 10^{14} - 10^{18} . Large datasets with experimentally characterized labeled data are quite valuable for constructing accurate models and libraries, so these tend to be closed-source and company-owned. Most current molecular generation applications utilize a subset of ZINC or ChemBL molecules. For this purpose, we propose a biological molecule benchmark set refined from the ZINC database.

The set is based on the ZINC Clean Leads collection. It contains 4,591,276 molecules in total, filtered by molecular weight in the range from 250 to 350 Daltons, a number of rotatable bonds not greater than 7, and XlogP less than or equal to 3.5. We removed molecules containing charged atoms or atoms besides C,

N, S, O, F, Cl, Br, H or cycles longer than 8 atoms. The molecules were filtered via medicinal chemistry filters (MCFs) and PAINS filters¹⁸.

Table 1. Datasets for generation tasks.

Dataset	Purpose	Size	URL
ZINC ^{19,20}	Commercially available compounds for virtual screening	980M	http://zinc15.docking.org/
ChEMBL ²¹	A manually curated database of bioactive molecules with drug-like properties	2M	https://www.ebi.ac.uk/chembl/
SureChEMBL ²²	Named compounds from chemical patents	17M	https://www.surechembl.org/search/
eMolecules	Purchasable molecules	18M	https://reaxys.emolecules.com/
SuperNatural ²³	Natural product molecules	330k	http://bioinformatics.charite.de/supernatural/
DrugBank	FDA approved drugs, experimental drugs, drugs available worldwide	10.5k	https://www.drugbank.ca/

Medicinal chemistry filters are used to discard compounds containing so-called "structural alerts". Molecules containing such moieties either bear unstable or reactive groups or undergo biotransformations resulting in the formation of toxic metabolites or intermediates. Herein, we present a list of routine MCFs for the rational pre-selection of compounds more appropriate for modern drug design and development. These include some electrophilic alkylating groups, such as Michael acceptors (MCF1-3), alkyl halides (MCF4), epoxide (MCF5), isocyanate (MCF6), aldehyde (MCF7), imine (Schiff base, MCF8), aziridine (MCF9) which are very liable for nucleophilic attack, e.g. by serine, lysine or amino group of cysteine. In many cases, it leads to unselective protein and/or DNA damage. Metabolism of hydrazine (MCF10) furnishes diazene intermediates (MCF11) which are also alkylating warheads. Monosubstituted furans (MCF12) and thiophenes (MCF13) are transformed into reactive intermediates via epoxidation. Their active metabolites irreversibly bind nucleophilic groups and modify proteins. Electrophilic aromatics (e.g. halopyridine, MCF14), oxidized anilines (MCF15) and disulfides (MCF16) are also highly reactive. *In vivo*, alkylators are trapped and inactivated by the thiol group of glutathione, which is a key natural antioxidant. Azides (MCF17) are highly toxic; compounds containing this functional group particularly cause genotoxicity. Aminals (MCF18) and acetals (MCF19) are frequently unstable and inappropriate in generated structures. In addition, virtual structures containing a large number of halogens (MCF20-22) should be excluded due to increased molecular weight and lipophilicity (insufficient solubility for oral administration), metabolic stability and toxicity. The detailed mechanism of toxicity for structure alerts mentioned above has been comprehensively described in^{24,25}.

The final dataset contains 1,936,962 molecular structures. For experiments, we also provide a training, test and scaffold test sets containing 250k, 10k, and 10k molecules respectively. The scaffold test set contains unique Bemis-Murcko scaffolds²⁶ that were not present in the training and test sets. We use this set to assess how well the model can generate previously unobserved scaffolds.

3. REPRESENTATIONS

Before training a generative or predictive model on molecular data, one has to represent compounds in a machine learning-friendly way. For generative tasks, we often would like to have a one-to-one mapping between the molecule and its representation to do a quick search in a lookup table, perform reconstruction, or sample new molecules. For the generative models considered in this work, we have focused on two primary forms of representation: sequences of tokens via SMILES^{27,28} and molecular graphs. Both representations rely on empirical principles of bonding, and a molecule is interpreted as an undirected graph where each atom is a node and the bonds are the edges. To reduce complexity, hydrogen atoms are treated implicitly because they are deduced from standard chemistry valence rules. A challenge when dealing with graphs is the graph isomorphism problem: without an explicit ordering of nodes, two graphs can map to the same structure and finding out whether they are equivalent is computationally demanding. This can be used for data augmentation purposes; but conversely, it has been argued that this representation degeneracy introduces noise to a model²⁹. In this section, we expand on these two representations and also elaborate on other alternatives that might be used for generative models.

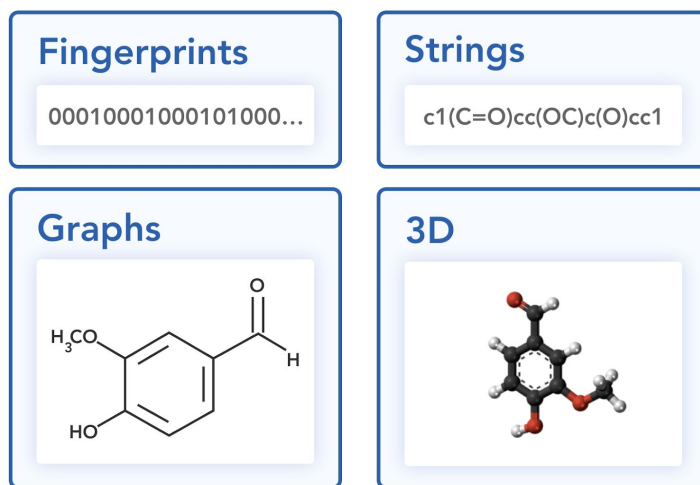


Figure 2. Different representations of a vanillin molecule

SMILES. Any graph can be transformed into a sequence of tokens by traversing its spanning tree and collecting all visited edges and nodes as tokens. For molecules, the Simplified Molecular Input Line System, or SMILES, defines grammar and syntax rules that are widely adopted in the chemistry community. In order to remove ambiguity, SMILES supports a canonical ordering (canonical SMILES)³⁰. Additionally, SMILES can also encode the stereochemistry by specifying special tokens for chirality (isomeric SMILES). A non-standard specification can also be adapted to include specific types of bonds, fragments, etc.

Much of the popularity behind SMILES in molecular generative models^{31–39} has been due to the fast adaptation of sequence modeling tools such as recurrent neural networks, attention mechanisms, and dilated convolutions, among others, to the text nature of SMILES. However, in a string format, we cannot preserve locality of atoms, and some atoms that are adjacent in the molecular graph can appear in distant positions in a string. Also, not every string with SMILES tokens is semantically correct, i.e., represents a valid molecule, so a neural network has to track distant relationships in SMILES, which leads to a lower number of valid strings. Some methods try to incorporate SMILES syntax into a network architecture to increase the fraction of valid molecules^{40,41}. There is also an International Chemical Identifier (InChI)⁴² format, which is a more verbose string representation, explicitly specifying a chemical formula, charges, hydrogens, and isotopes.

Molecular graphs. In a machine learning context, graphs are normally represented via sparse adjacency matrices with values corresponding to the presence or absence of edges between vertices. These matrices are augmented with node and edge feature vectors since nodes and edges in molecular graphs are likely to include physical properties related to the atoms and bonds. Often these are represented as sparse tensors⁴³.

There are multiple ways of processing and taking into account information defined on a graph, and so several approaches have been proposed such as Graph Convolutional Networks⁴⁴, Weave Networks¹⁵, and Message Passing Networks⁴⁵. The molecular graph can be represented implicitly as an adjacency matrix with different atoms encoded along certain dimensions of the tensor; this approach has been successfully used in the MolGAN model⁴⁶ for the QM9 dataset⁴⁷. Another approach for treating graphs was introduced with the junction tree model⁴⁸, which, instead of modeling a molecular graph as an atom-wise graph, interprets each molecule as having been built from subgraphs chosen out of a vocabulary of fragments.

3D structure and alternative representations. For a long time, one of the most common representations for molecular structures has been a *fingerprint*, a fixed-length vector indicating the presence or absence of a chemical environment^{49,50}. Fingerprints are not typically invertible but can be used for fast screening by similarity to available in-house compounds. Kadurin et al.³⁸ implemented VAE and AAE models based on Molecular Access System (MACCS) fingerprints to screen for novel compounds with the desired effect. Polykovskiy et al.⁵¹ proposed a generative model for creating molecular structures for a given fingerprint, training a simple generator on fingerprints and then transforming them into molecules with a separate model. However, fingerprints often lack biological relevance and do not fit into the process of designing novel compounds.

One shortcoming of using molecular graphs and SMILES to model chemical and physical phenomena is that they represent a description of molecules on the level of atoms. A complete description of a molecule will require to take into account their 3D coordinates, symmetries with respect to the Schrödinger equation, and possibly its electrons. This is a current open research problem, and therefore we would like to draw attention to other works that involve alternative representations for molecules and could be potentially used or expanded for generative models.

One promising direction lies in a wavefunction or electronic density representation of molecules; these should in principle contain all information needed for an exact description of the physics and chemistry of a molecule. An initial approximation was introduced with the help of invertible hamiltonians via Coulomb matrices⁵² that contain pairwise Coulomb interactions between atoms. Their generalization can be seen as

tensors that encode multiple symmetries and physical properties of atoms⁵³. The use of electronic densities has also been explored for prediction⁵⁴.

Another representation has relied on position molecules within a 3D grid space, often with channels for different types of atoms, where a voxel is non-zero when it contains an atom. This representation is quite flexible since it can also incorporate information about the binding position in an active site of a protein^{55,56}. One major challenge of this representation is sparsity; for this purpose, Kuzminykh et al.⁵⁷ proposed an invertible smoothing transformation to reduce sparsity in the 3D space. Building generative models on 3D representations remains an open problem. One of the current approaches that allows to work directly in the 3D space is providing 3D coordinates to graph nodes or SMILES atoms.

4. METRICS

Generative models are supposed to produce a wide variety of different samples. Therefore, to evaluate generative models one has to compare *sets* of generated molecules, looking for coverage of the ground truth, diversity among generated objects, and similarity between various statistical properties of the generated set and the reference set. To this purpose, we have utilized five metrics that can be used to compare a generated set of molecules G and a reference set of molecules R : fragment similarity, scaffold similarity, nearest neighbor similarity (based on Morgan structural fingerprints and Gobby 2D topological fingerprints), internal diversity, and Fréchet ChEMBLNet Distance. We also present a set of auxiliary metrics useful for the drug design process but could be extended for other applications.

Fragment similarity (Frag) is defined as the cosine distance between vectors of fragment frequencies. For a set of molecules M , its fragment frequency vector f_M has a size equal to the size of the vocabulary of all chemical fragments in the dataset, and elements of f_S represent frequencies with which the corresponding fragments appear in S . The distance is then defined as

$$Frag(G, R) = 1 - \cos(f_S, f_R),$$

where molecules in both G and R are fragmented using the BRICS algorithm⁵⁸ implemented in RDKit⁵⁹. This metric shows the similarity of two sets of molecules at the level of chemical fragments.

Scaffold similarity (Scaff) is calculated in a similar way, as cosine similarity between the vectors S_G and S_R that represent frequencies of scaffolds in sets of molecules G and R :

$$Scaff(G, R) = 1 - \cos(s_S, s_R),$$

Scaffolds are derived from the molecules by removing side chain atoms using the Bemis–Murcko algorithm²⁶, also implemented in RDKit⁵⁹. The purpose of this metric is to show how similar are the scaffolds in generated and reference datasets. Note that in both fragment and scaffold similarity the comparison is at a substructure level but not molecule level, i.e. it is possible to have a distance of 0 (identical) with two different sets of molecules, as long as their substructure counts are the same.

Nearest neighbor similarity (SNN) is the average Tanimoto similarity $T(m_G, m_R)$ (also known as the Jaccard index) between a molecule m_G from the generated set G and its nearest neighbor molecule m_R in the reference dataset R :

$$SNN(G, R) = \frac{1}{|G|} \sum_{m_G \in G} \max_{m_R \in R} T(m_G, m_R),$$

Where m_R and m_G are some representations of the molecules as bit strings (fingerprints); the resulting similarity metric shows how generated molecules are similar to reference molecules in terms of the chemical structures that are encoded in these fingerprints. In this work, we used standard Morgan⁶⁰ fingerprints with radius 2. This representation is useful for a general analysis of the chemical space considering the constant search for novel scaffolds and chemotypes which is an essential part of the modern drug discovery process.

However, although molecules with similar chemical structures tend to possess the same biological response, there are more common features called *pharmacophores* that are responsible for biological activity. It has been shown that structurally diverse ligands with common pharmacophore hypothesis can bind to the same receptor site⁶¹. Therefore, nearest neighbor similarity calculated using 2D pharmacophore fingerprints⁵⁰ can be beneficial when comparing two sets of molecules with regards to the biological targets they can bind to.

Internal diversity (Div)⁶² assesses the chemical diversity within the generated set of molecules G .

$$Div(G) = 1 - \frac{1}{|G|^2} \sum_{m_1, m_2 \in G} T(m_1, m_2).$$

While SNN measures the dissimilarity to the reference dataset (external diversity), the internal diversity metric evaluates the generated molecules. This metric detects a common failure case of generative models—mode collapse. With mode collapse the model produces a limited variety of samples, ignoring some areas of chemical space. A higher value of the metric corresponds to higher diversity in the generated set.

Fréchet ChemNet Distance (FCD)⁶³ is calculated using the last layer of the deep neural network *ChemNet* trained to predict the biological activities of drugs. This last layer contains a Gaussian-distributed vector representation of the molecules that takes into account both chemical and biological properties of the compounds. For two sets of molecules G and R , it is defined as

$$(G, R) = \|\mu_G - \mu_R\|^2 + Tr(\Sigma_G + \Sigma_R - 2(\Sigma_G \Sigma_R)^{1/2}),$$

where μ_G , μ_R are mean vectors and Σ_G , Σ_R are covariance matrices of the activations on the penultimate layer of *ChemNet* on the sets G and R respectively.

We believe that these five metrics provide a good coverage of various desirable properties of a set of generated molecules, and we propose to use them as standard metrics for the comparison of different generative models for molecular fingerprints and structures.

Auxiliary Metrics. For evaluation purposes, we have also included utilities for computing auxiliary metrics that represent qualities that are commonly used for small molecule drug discovery.

- **Molecular weight (MW):** the sum of atomic weights in a molecule.
- **LogP:** the water-octanol partition coefficient, a property that measures how likely a molecule is able to mix with water. Computed via RDKit’s Crippen⁶⁴ function.
- **Synthetics Accessibility Score (SA):** a heuristic estimate of how hard (10) or how easy (1) it is to synthesize a given molecule. SAscore is based on a combination of fragment contributions and a complexity penalty⁶⁵.
- **Quantitative Estimation of Drug-likeness (QED):** a 0 to 1 float value estimating how likely a molecule is a viable candidate for a drug. QED is meant to capture the abstract notion of aesthetics in medicinal chemistry⁶⁶.

- **Natural Product-likeness Score (NP):** a numerical estimate that can be used to determine if a molecule is likely to be a natural product (0...5), a drug molecule (-3...3) or a synthetic product (-5...0). This score is calculated from several substructure descriptors and comparing them to the properties of other distributions of molecules⁶⁷.

For comparison purposes we use the Frèchet distance to measure the distance between distributions of molecules in relation to these properties; this allows for a one-number comparison between complicated distributions. Alternatively, distributions of molecules can be compared in a simplified manner by looking at the mean and variance of properties.

Baseline models. In the current version of MOSES, we implemented several deep learning models that cover different approaches to molecule generation problem such as language models modeled as character-level recurrent neural networks (CharRNN)^{32,63}, Variational and Adversarial Autoencoders (VAE^{68,69,70}, AAE^{71,69,51}), Junction Tree Variational Autoencoders (JT-VAE)⁴⁸, and Objective-reinforced generative adversarial network (ORGAN)^{34,72}. These baseline models are trained in an unsupervised or semi-supervised fashion. Most models are based on the SMILES representation of a molecule and as such will typically incorporate sequence modeling tools such as recurrent neural networks (RNN) with different types of cells. There are many new models coming out dealing with other representation of molecules such as the JT-VAE which works with molecular graphs as tensors. Although more models will be added, we believe the current coverage in the collection is sufficient for good comparison of any arbitrary new model.

Model comparison can be challenging since different training parameters (number of epochs, batch size, learning rate, initial state, optimizer) and architecture hyperparameters (hidden layer dimension, number of layers etc.) can significantly alter their performance. For each model, we attempted to preserve its original architecture as published and tweaked hyperparameters to improve performance. We used random search over 100 architectures for every model and selected the architecture that produced the highest chemical validity. For models with the same validity, we chose models with the highest uniqueness. All models are implemented with Python 3 utilizing the PyTorch⁷³ machine learning framework. Next, we briefly introduce these models.

Character-level recurrent neural networks (CharRNN)³² treats the task of generating SMILES as a language model attempting to learn the statistical structure of SMILES syntax by training it on a large corpus of SMILES (Figure 3). Model parameters are optimized using maximum likelihood estimation (MLE). CharRNN is implemented using Long Short-Term Memory⁷⁴ RNN cells stacked into three layers with hidden dimension 600 each. To prevent overfitting, a dropout layer⁷⁵ is added between intermediate layers with dropout probability of 0.2. Softmax is utilized as an output layer. Training is done with a batch size of 64, using the Adam⁷⁶ optimizer with a learning rate of 10^{-3} for 50 epochs.

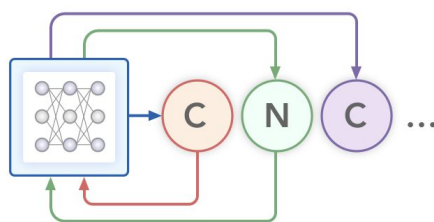


Figure 3. CharRNN model. A model is trained by maximizing the likelihood of known molecules.

Variational autoencoder (VAE) is a framework for training two neural networks—an encoder and a decoder—to learn a mapping from high-dimensional data representation into a lower-dimensional space and back. The lower-dimensional space is called the latent space, which is often a continuous vector space with normally distributed latent representation. VAE parameters are optimized to encode and decode data by minimizing the reconstruction loss while also minimizing a KL-divergence term arising from the variational approximation that can loosely be interpreted as a regularization term (Figure 4). Since molecules are discrete objects, properly trained VAE defines an invertible continuous representation of a molecule.

A VAE-based architecture for the molecular generation was initially proposed by Gómez-Bombarelli et al.⁶⁸, and alternative architectures have been proposed by Kadurin et al.⁶⁹ and Blaschke et al.⁷⁰. We combine aspects from both implementations in MOSES. Utilizing a bidirectional⁷⁷ Gated Recurrent Unit (GRU)⁷⁸ with a linear output layer as an encoder. The decoder is a 3-layer GRU RNN of 512 hidden dimensions with intermediate dropout layers with dropout probability 0.2. Training is done with a batch size of 128, utilizing a gradient clipping of 50, KL-term weight of 1, and optimized with Adam with a learning rate of 3×10^{-4} for 50 epochs.

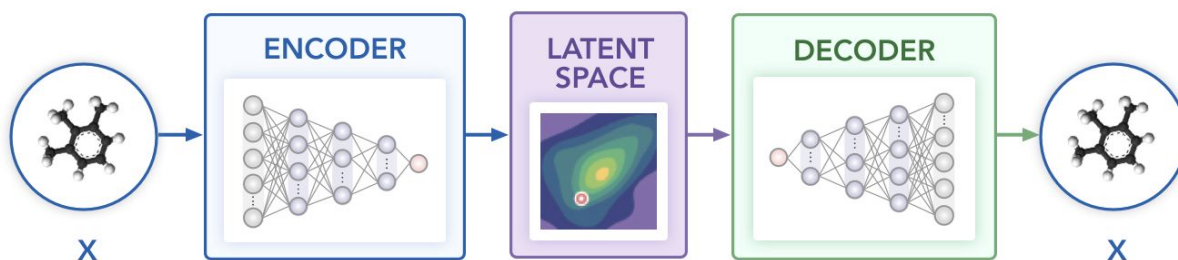


Figure 4. Autoencoder-based models. VAE/AAE forms a specific distribution in the latent space.

Adversarial Autoencoders (AAE)⁷¹ combine the idea of VAE with that of adversarial training as found in GAN. One of the main drawbacks of VAE is the KL divergence term that has a closed-form analytical solution only for a handful of distributions. In AAE, the KL divergence term is avoided by training a discriminator network to predict whether a given sample came from the latent space of the AE or from a

prior distribution. Parameters are optimized to minimize the reconstruction loss and to minimize the discriminator loss. Kadurin et al.⁶⁹ applied AAE architecture to the drug generation task. The model consists of an encoder with a 1-layer bidirectional LSTM with 380 hidden dimensions, a decoder with a 2-layer LSTM with 640 hidden dimensions and a shared embedding of size 32. The latent space is of dimension 640, and the discriminator networks is a 2-layer fully connected neural network with 640 and 256 nodes respectively, utilizing the ELU activation function⁷⁹. Training is done with a batch size of 128, with the Adam optimizer using a learning rate of 10^{-3} for 25 epochs.

Junction Tree VAE (JT-VAE)⁸⁰ is one of the first deep generative models that explicitly made use of a graph representation of molecules. The JT-VAE generates molecules in two phases by exploiting valid subgraphs as components. In the first phase, it generates a tree-structured object (a junction tree) whose role is to represent the scaffold of subgraph components and their coarse relative arrangements. The components are valid chemical substructures automatically extracted from the training set using tree decomposition and are then used as building blocks. In the second phase, the subgraphs (nodes of the tree) are assembled together into a coherent molecular graph.

Training is done with a batch size of 40, with the Adam optimizer utilizing a learning rate of 10^{-3} for 5 epochs. Hyperparameters are based on the original paper: hidden layer dimension 450, a latent space of dimension 56 and the message passing graph of depth 3. The KL term was taken into consideration starting from the second epoch, allowing one epoch for just training the VAE part. The KL term weight was 0.0005.

Objective-reinforced generative adversarial network (ORGAN)^{34,72} is a sequence generation model based on adversarial training that aims at generating discrete sequences that emulate a data distribution while biasing the generation process towards some desired objective rewards using reinforcement learning. ORGAN incorporates at least 2 networks: a generator network and a discriminator network. The goal of the generator network is to create synthetic data examples that are indistinguishable from the empirical data distribution. The discriminator exists to learn to distinguish synthetic from real data samples. Both models are trained in alternation (Figure 5).

To properly train a GAN, the gradient must be backpropagated between the generator and discriminator model, which is not possible when the data samples come from a discrete distribution such as multinomial since discrete distributions are non-differentiable. SeqGAN¹⁰ proposed to learn a policy gradient that can be backpropagated and calculated using the REINFORCE⁸¹ algorithm. ORGAN extended this framework to include other reward functions besides the discriminator. Reinforcement is done with an N-depth Monte Carlo tree search, and the reward is a weighted sum of probabilities from the discriminator and objective reward. Both the generator and discriminator are pre-trained for 250 and 50 epochs respectively, and then jointly trained for 100 epochs utilizing the Adam optimizer with a learning rate of 10^{-4} . In the experiments, we used chemical validity and uniqueness as rewards.

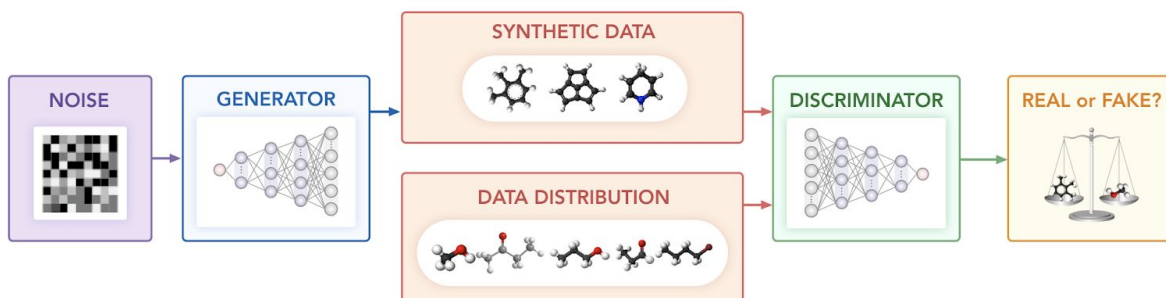


Figure 5. GAN-based generative models. The discriminator is trained to distinguish generated objects from real ones.

5. RESULTS

We trained baseline models on the proposed dataset and tuned hyperparameters independently to achieve maximal validity and uniqueness. In Table 2, we provide main metrics implemented within the MOSES platform. According to the experiments, VAE outperforms other architectures on the Fréchet ChemNet distance metric (FCD), suggesting the VAE describe the chemical space better than other models. AAE is better in discovering novel scaffolds as suggested by *Scaff/TestSF* metric. All models successfully learn SMILES syntax, as indicated by *Valid* metric. In Figure 6, we compare distributions of chemical properties in generated and reference sets. We notice, that most of the models match the shape of the distribution, although some models (AAE and JTN-VAE) expose bias towards more complex molecules, as SA score is on average higher for generated molecules than for the reference dataset.

Table 2. Metrics for generative models. The most up-to-date version of the comparison table can be found at <https://github.com/molecularsets/>.

	Valid (↑)	U@1k (↑)	U@10k (↑)	FCD (↓)		SNN (↓)		Frag (↑)		Scaff (↑)		IntDiv (↑)	Filters (↑)
				Test	TestS F	Test	TestSF	Test	TestSF	Test	TestSF		
CharRNN	0.96	1	0.999	0.3233	0.836	0.461	0.449	0.998	0.9962	0.796	0.128	0.856	0.992
VAE	0.95	1	0.999	0.254	0.696	0.468	0.455	0.998	0.9963	0.828	0.093	0.855	0.993
AAE	0.93	1	1	1.351	1.859	0.419	0.411	0.987	0.9852	0.664	0.154	0.853	0.976
ORGAN	0.87	0.991	0.926	1.575	2.431	0.475	0.459	0.99	0.9883	0.784	0.063	0.853	0.994
JT-VAE	1	0.998	0.997	4.377	4.63	0.391	0.39	0.968	0.9699	0.387	0.116	0.85	0.957

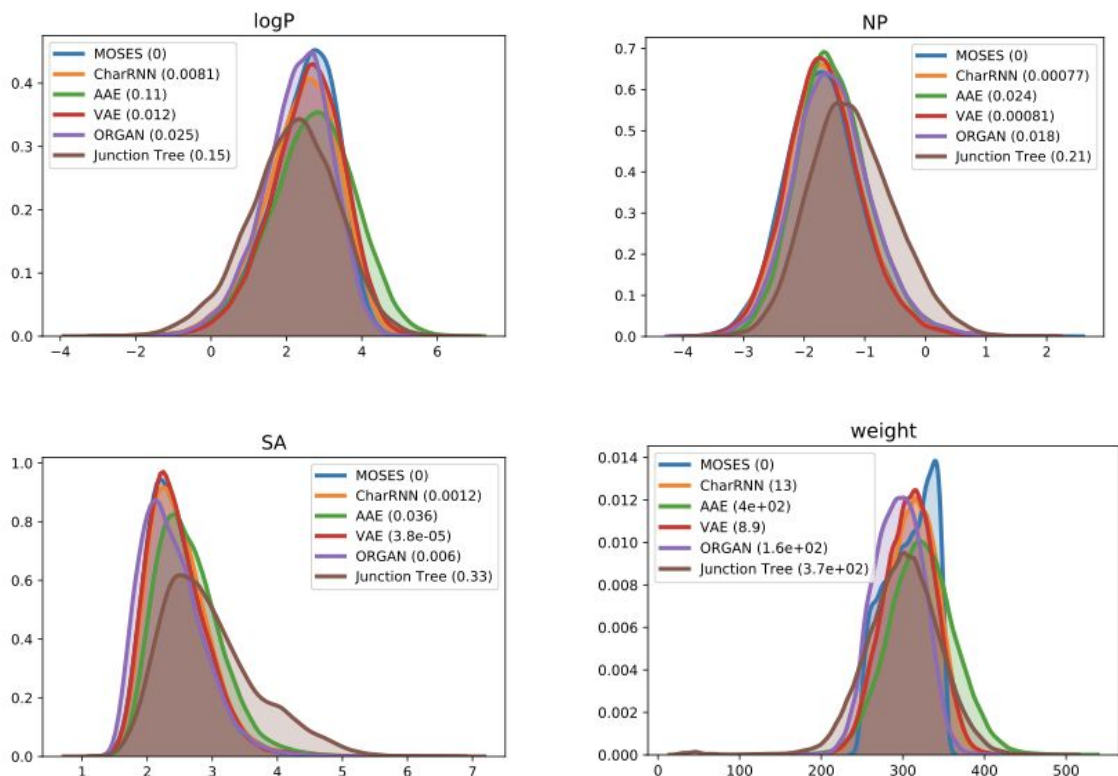


Figure 6. Distribution of chemical properties for MOSES dataset and sets of generated molecules. In brackets—Fréchet distance to MOSES dataset.

6. DISCUSSION

With MOSES, we have designed a molecular generation benchmark platform that combines several existing state-of-the-art baseline models and several evaluation metrics. This platform should allow for a fair and comprehensive comparison of new generative models. Providing a one-size-fits-all solution for a given molecular application is not possible since the constraints, chemistry, and properties of interest are highly varied and very specific for a given context. We design MOSES as the first baseline of comparison, providing metrics that allow taking into account several perspectives relevant to molecular generation. For future work on this project, we will keep extending the MOSES repository with new baseline models, updated evaluation tables, as well as incorporating new evaluation metrics.

We also wish to highlight and re-emphasize several research directions and challenges that future generative models and efforts should tackle.

- **Organic material datasets.** While most easily available datasets cover biological contexts, there is a need for large high-quality datasets corresponding to organic materials for redox flow batteries, light emitting diodes, solar cell, dyes, polymers and copolymers, odorants, crop protectants, and food preservatives.
- **Non-atom centric representations of molecules.** Most generative models have focused on the usage of molecular graph either explicitly or as SMILES. To be able to describe more accurately

and completely molecular processes we might need representations that include information related to electrons or 3D structure of a molecule.

- **Hierarchical representations of molecules.** As noted with JT-VAE, a hierarchical model might be able to leverage structure at different scales (atoms, fragments, etc.). This might prove important towards moving from small molecules to proteins, where the number of atoms can be on the order of thousands. Structured representations might benefit from reduced complexity, in processing time but also for prediction.
- **Better and more general metrics.** Current auxiliary metrics has been developed around heuristics and rules of medicinal chemistry, often validated with small datasets due to the lack of publicly available datasets. To build better guided generative models we need more accurate metrics that go beyond just medicinal chemistry. Measuring the ease of synthesizability and cost of synthesis of a molecule, incorporating reaction path between commercially available reactants and natural products is important⁸², as well as measuring reliably solubility and miscibility between materials, in a variety of molecules environments⁸³.
- **Guided and biased generation.** There have been several demonstrations of being able to bias the generative process of models using reinforcement learning^{72,84,85}, often these methods (e.g. Monte Carlo Tree Search) are data intensive, so more efficient RL optimization methods are needed. For areas of application that deserve attention are the generation of symmetry-point group preserving molecules and navigation around patented molecular space. The former is important for planning and simplifying synthesis, the latter for promoting or avoiding certain types of substructures.

We hope this work enables future researchers interested in tackling pressing molecular and material challenges.

REFERENCES

1. Tabor, D. P. *et al.* Accelerating the discovery of materials for clean energy in the era of smart automation. *Nature Reviews Materials* **3**, 5–20 (2018).
2. Lee, S.-I. *et al.* A machine learning approach to integrate big data for precision medicine in acute myeloid leukemia. *Nat. Commun.* **9**, 42 (2018).
3. Reymond, J.-L. The Chemical Space Project. *Acc. Chem. Res.* **48**, 722–730 (2015).
4. Kirkpatrick, P. & Ellis, C. Chemical space. *Nature* **432**, 823–823 (2004).
5. Le, T. C. & Winkler, D. A. Discovery and Optimization of Materials Using Evolutionary Approaches. *Chem. Rev.* **116**, 6107–6132 (2016).
6. Hu, X., Beratan, D. N. & Yang, W. Emergent strategies for inverse molecular design. *Sci. China B* **52**, 1769–1776 (2009).
7. Curtarolo, S. *et al.* The high-throughput highway to computational materials design. *Nat. Mater.* **12**, 191–201 (2013).
8. Pyzer-Knapp, E. O., Suh, C., Gómez-Bombarelli, R., Aguilera-Iparraguirre, J. & Aspuru-Guzik, A. What Is High-Throughput Virtual Screening? A Perspective from Organic Materials Discovery. *Annu. Rev. Mater. Res.* **45**, 195–216 (2015).
9. Karras, T., Aila, T., Laine, S. & Lehtinen, J. Progressive Growing of GANs for Improved Quality, Stability, and Variation. *arXiv [cs.NE]* (2017).
10. Yu, L., Zhang, W., Wang, J. & Yu, Y. SeqGAN: Sequence Generative Adversarial Nets with Policy Gradient. *arXiv [cs.LG]* (2016).

11. Killoran, N., Lee, L. J., DeLong, A., Duvenaud, D. & Frey, B. J. Generating and designing DNA with deep generative models. *arXiv [cs.LG]* (2017).
12. Sanchez-Lengeling, B. & Aspuru-Guzik, A. Inverse molecular design using machine learning: Generative models for matter engineering. *Science* **361**, 360–365 (2018).
13. LeCun, Y. The MNIST database of handwritten digits. <http://yann.lecun.com/exdb/mnist/>
14. Deng, J. *et al.* ImageNet: A Large-Scale Hierarchical Image Database. in *CVPR09* (2009).
15. Wu, Z. *et al.* MoleculeNet: a benchmark for molecular machine learning. *Chem. Sci.* **9**, 513–530 (2018).
16. Schneider, N., Lowe, D. M., Sayle, R. A., Tarselli, M. A. & Landrum, G. A. Big Data from Pharmaceutical Patents: A Computational Analysis of Medicinal Chemists' Bread and Butter. *J. Med. Chem.* **59**, 4385–4402 (2016).
17. Walters, W. P. Virtual Chemical Libraries. *J. Med. Chem.* (2018). doi:10.1021/acs.jmedchem.8b01048
18. Baell, J. B. & Holloway, G. A. New substructure filters for removal of pan assay interference compounds (PAINS) from screening libraries and for their exclusion in bioassays. *J. Med. Chem.* **53**, 2719–2740 (2010).
19. Irwin, J. J. & Shoichet, B. K. ZINC – A Free Database of Commercially Available Compounds for Virtual Screening ZINC - A Free Database of Commercially Available Compounds for Virtual Screening. *J. Chem. Inf. Model.* **45**, 177–182 (2005).
20. Sterling, T. & Irwin, J. J. ZINC 15 - Ligand Discovery for Everyone. *J. Chem. Inf. Model.* **55**, 2324–2337 (2015).
21. Gaulton, A. *et al.* The ChEMBL database in 2017. *Nucleic Acids Res.* **45**, D945–D954 (2017).
22. Papadatos, G. *et al.* SureChEMBL: a large-scale, chemically annotated patent document database. *Nucleic Acids Res.* **44**, D1220–8 (2016).
23. Banerjee, P. *et al.* Super Natural II--a database of natural products. *Nucleic Acids Res.* **43**, D935–9 (2015).
24. Kalgutkar, A. S. *et al.* A comprehensive listing of bioactivation pathways of organic functional groups. *Curr. Drug Metab.* **6**, 161–225 (2005).
25. Kalgutkar, A. S. & Soglia, J. R. Minimising the potential for metabolic activation in drug discovery. *Expert Opin. Drug Metab. Toxicol.* **1**, 91–142 (2005).
26. Bemis, G. W. & Murcko, M. A. The properties of known drugs. 1. Molecular frameworks. *J. Med. Chem.* **39**, 2887–2893 (1996).
27. Weininger, D. SMILES, a chemical language and information system. 1. Introduction to methodology and encoding rules. *J. Chem. Inf. Comput. Sci.* **28**, 31–36 (1988).
28. Weininger, D., Weininger, A. & Weininger, J. L. SMILES. 2. Algorithm for generation of unique SMILES notation. *J. Chem. Inf. Comput. Sci.* **29**, 97–101 (1989).
29. von Lilienfeld, O. A. First principles view on chemical compound space: Gaining rigorous atomistic control of molecular properties. *Int. J. Quantum Chem.* **113**, 1676–1689 (2013).
30. O'Boyle, N. M. Towards a Universal SMILES representation - A standard method to generate canonical SMILES based on the InChI. *J. Cheminform.* **4**, 22 (2012).
31. Popova, M., Isayev, O. & Tropsha, A. Deep reinforcement learning for de novo drug design. *Sci Adv* **4**, eaap7885 (2018).
32. Segler, M. H. S., Kogej, T., Tyrchan, C. & Waller, M. P. Generating Focused Molecule Libraries for Drug Discovery with Recurrent Neural Networks. *ACS Cent Sci* **4**, 120–131 (2018).
33. Jaques, N. *et al.* Sequence Tutor: Conservative Fine-Tuning of Sequence Generation Models with KL-control. *arXiv* (2016).
34. Guimaraes, G. L., Sanchez-Lengeling, B., Farias, P. L. C. & Aspuru-Guzik, A. Objective-Reinforced Generative Adversarial Networks (ORGAN) for Sequence Generation Models. *arXiv* (2017).

35. Olivecrona, M., Blaschke, T., Engkvist, O. & Chen, H. Molecular de-novo design through deep reinforcement learning. *J. Cheminform.* **9**, 48 (2017).
36. Kang, S. & Cho, K. Conditional Molecular Design with Deep Generative Models. *J. Chem. Inf. Model.* (2018). doi:10.1021/acs.jcim.8b00263
37. Yang, X., Zhang, J., Yoshizoe, K., Terayama, K. & Tsuda, K. ChemTS: an efficient python library for de novo molecular generation. *Sci. Technol. Adv. Mater.* **18**, 972–976 (2017).
38. Kadurin, A., Nikolenko, S., Khrabrov, K., Aliper, A. & Zhavoronkov, A. druGAN: An Advanced Generative Adversarial Autoencoder Model for de Novo Generation of New Molecules with Desired Molecular Properties in Silico. *Mol. Pharm.* **14**, 3098–3104 (2017).
39. Putin, E. *et al.* Adversarial Threshold Neural Computer for Molecular de Novo Design. *Mol. Pharm.* **15**, 4386–4397 (2018).
40. Kusner, M. J., Paige, B. & Hernández-Lobato, J. M. Grammar Variational Autoencoder. *arXiv [stat.ML]* (2017).
41. Dai, H., Tian, Y., Dai, B., Skiena, S. & Song, L. Syntax-Directed Variational Autoencoder for Structured Data. *arXiv [cs.LG]* (2018).
42. The IUPAC International Chemical Identifier (InChI). *Chemistry International -- Newsmagazine for IUPAC* **31**, (2009).
43. You, J., Ying, R., Ren, X., Hamilton, W. & Leskovec, J. GraphRNN: Generating Realistic Graphs with Deep Auto-regressive Models. in *International Conference on Machine Learning* 5694–5703 (2018).
44. Duvenaud, D. *et al.* Convolutional Networks on Graphs for Learning Molecular Fingerprints. *arXiv [cs.LG]* (2015).
45. Gilmer, J., Schoenholz, S. S., Riley, P. F., Vinyals, O. & Dahl, G. E. Neural Message Passing for Quantum Chemistry. *arXiv [cs.LG]* (2017).
46. De Cao, N. & Kipf, T. MolGAN: An implicit generative model for small molecular graphs. *arXiv [stat.ML]* (2018).
47. Ramakrishnan, R., Dral, P. O., Rupp, M. & von Lilienfeld, O. A. Quantum chemistry structures and properties of 134 kilo molecules. *Scientific Data* **1**, 140022 (2014).
48. Jin, W., Barzilay, R. & Jaakkola, T. Junction Tree Variational Autoencoder for Molecular Graph Generation. in *Proceedings of the 35th International Conference on Machine Learning* (eds. Dy, J. & Krause, A.) **80**, 2323–2332 (PMLR, 2018).
49. Rogers, D. & Hahn, M. Extended-connectivity fingerprints. *J. Chem. Inf. Model.* **50**, 742–754 (2010).
50. Gobbi, A. & Poppinger, D. Genetic optimization of combinatorial libraries. *Biotechnol. Bioeng.* **61**, 47–54 (1998).
51. Polykovskiy, D. *et al.* Entangled Conditional Adversarial Autoencoder for de Novo Drug Discovery. *Mol. Pharm.* (2018). doi:10.1021/acs.molpharmaceut.8b00839
52. Rupp, M., Tkatchenko, A., Müller, K.-R. & von Lilienfeld, O. A. Fast and accurate modeling of molecular atomization energies with machine learning. *Phys. Rev. Lett.* **108**, 058301 (2012).
53. Hy, T. S., Trivedi, S., Pan, H., Anderson, B. M. & Kondor, R. Predicting molecular properties with covariant compositional networks. *J. Chem. Phys.* **148**, 241745 (2018).
54. Eickenberg, M., Exarchakis, G., Hirn, M., Mallat, S. & Thiry, L. Solid harmonic wavelet scattering for predictions of molecule properties. *J. Chem. Phys.* **148**, 241732 (2018).
55. Wallach, I., Dzamba, M. & Heifets, A. AtomNet: A Deep Convolutional Neural Network for Bioactivity Prediction in Structure-based Drug Discovery. *arXiv [cs.LG]* (2015).
56. Gomes, J., Ramsundar, B., Feinberg, E. N. & Pande, V. S. Atomic Convolutional Networks for Predicting Protein-Ligand Binding Affinity. *arXiv [cs.LG]* (2017).
57. Kuzminykh, D. *et al.* 3D Molecular Representations Based on the Wave Transform for

- Convolutional Neural Networks. *Mol. Pharm.* (2018). doi:10.1021/acs.molpharmaceut.7b01134
58. Degen, J., Wegscheid-Gerlach, C., Zaliani, A. & Rarey, M. On the art of compiling and using ‘drug-like’ chemical fragment spaces. *ChemMedChem* **3**, 1503–1507 (2008).
 59. Landrum, G. RDKit: Open-source cheminformatics. Available at: <http://www.rdkit.org/>.
 60. Morgan, H. L. The Generation of a Unique Machine Description for Chemical Structures-A Technique Developed at Chemical Abstracts Service. *J. Chem. Doc.* **5**, 107–113 (1965).
 61. Van Drie, J. H. Monty Kier and the origin of the pharmacophore concept. *Internet Electron. J. Mol. Des* **6**, 271–279 (2007).
 62. Benhenda, M. ChemGAN challenge for drug discovery: can AI reproduce natural chemical diversity? *CoRR* **abs/1708.08227**, (2017).
 63. Preuer, K., Renz, P., Unterthiner, T., Hochreiter, S. & Klambauer, G. Fréchet ChemNet Distance: A Metric for Generative Models for Molecules in Drug Discovery. *J. Chem. Inf. Model.* **58**, 1736–1741 (2018).
 64. Wildman, S. A. & Crippen, G. M. Prediction of Physicochemical Parameters by Atomic Contributions. *J. Chem. Inf. Comput. Sci.* **39**, 868–873 (1999).
 65. Ertl, P. & Schuffenhauer, A. Estimation of synthetic accessibility score of drug-like molecules based on molecular complexity and fragment contributions. *J. Cheminform.* **1**, 8 (2009).
 66. Bickerton, G. R., Paolini, G. V., Besnard, J., Muresan, S. & Hopkins, A. L. Quantifying the chemical beauty of drugs. *Nat. Chem.* **4**, 90–98 (2012).
 67. Ertl, P., Roggo, S. & Schuffenhauer, A. Natural product-likeness score and its application for prioritization of compound libraries. *J. Chem. Inf. Model.* **48**, 68–74 (2008).
 68. Gómez-Bombarelli, R. *et al.* Automatic Chemical Design Using a Data-Driven Continuous Representation of Molecules. *ACS Central Science* **4**, 268–276 (2018).
 69. Kadurin, A. *et al.* The cornucopia of meaningful leads: Applying deep adversarial autoencoders for new molecule development in oncology. *Oncotarget* **8**, 10883–10890 (2017).
 70. Blaschke, T., Olivecrona, M., Engkvist, O., Bajorath, J. & Chen, H. Application of Generative Autoencoder in De Novo Molecular Design. *Mol. Inform.* **37**, (2018).
 71. Makhzani, A., Shlens, J., Jaitly, N., Goodfellow, I. & Frey, B. Adversarial Autoencoders. *arXiv [cs.LG]* (2015).
 72. Sanchez-Lengeling, B., Outeiral, C., Guimaraes, G. L. & Aspuru-Guzik, A. Optimizing distributions over molecular space. An Objective-Reinforced Generative Adversarial Network for Inverse-design Chemistry (ORGANIC). (2017). doi:10.26434/chemrxiv.5309668.v3
 73. Paszke, A. *et al.* Automatic differentiation in PyTorch. (2017).
 74. Hochreiter, S. & Schmidhuber, J. Long short-term memory. *Neural Comput.* **9**, 1735–1780 (1997).
 75. Srivastava, N. Improving neural networks with dropout. (University of Toronto, 2013).
 76. Kingma, D. P. & Lei Ba, J. Adam: A Method of Stochastic Optimization. *ICLR* 1–15 (2015).
 77. Schuster, M. & Paliwal, K. K. Bidirectional recurrent neural networks. *IEEE Trans. Signal Process.* **45**, 2673–2681 (1997).
 78. Cho, K. *et al.* Learning Phrase Representations using RNN Encoder-Decoder for Statistical Machine Translation. *arXiv [cs.CL]* (2014).
 79. Clevert, D.-A., Unterthiner, T. & Hochreiter, S. Fast and Accurate Deep Network Learning by Exponential Linear Units (ELUs). *arXiv [cs.LG]* (2015).
 80. Jin, W., Barzilay, R. & Jaakkola, T. Junction Tree Variational Autoencoder for Molecular Graph Generation. *arXiv [cs.LG]* (2018).
 81. Williams, R. J. Simple statistical gradient-following algorithms for connectionist reinforcement learning. *Mach. Learn.* **8**, 229–256 (1992).
 82. Palazzolo, A. M. E., Simons, C. L. W. & Burke, M. D. The natural productome. *Proc. Natl. Acad. Sci. U. S. A.* **114**, 5564–5566 (2017).

83. Sanchez-Lengeling, B. *et al.* A Bayesian Approach to Predict Solubility Parameters. *Adv. Theory Simul.* **17**, 1800069 (2018).
84. Segler, M. H. S., Preuss, M. & Waller, M. P. Planning chemical syntheses with deep neural networks and symbolic AI. *Nature* **555**, 604–610 (2018).
85. Putin, E. *et al.* Reinforced Adversarial Neural Computer for de Novo Molecular Design. *J. Chem. Inf. Model.* **58**, 1194–1204 (2018).